

AN OXYGEN TRANSPORT MODEL OF HUMAN BONE MARROW FOR HEMOLYTIC SICKLE CELL ANEMIA

M. A. Islam*

Department of Chemical Engineering and Applied Chemistry
University of Toronto, 200 College Street, Toronto ON, M5S 3E5, Canada

R. Kumar

Petrofac Engineering, 76-86 Chertsey Road, Woking Surrey, GU21 5BJ, UK

Abstract

The human bone marrow (BM) is a complicated tissue with intricate vascular and heterogeneous extravascular (tissue) architecture. Oxygen is an important modulator of differentiation and proliferation of the BM hematopoietic cells under normal and pathological conditions. Currently, due to the inaccessibility of the BM, it is not possible to measure the spatial distribution of the oxygen tension (concentration) levels in the tissue. Thus, the present treatise utilizes mathematical modeling to offer a greater insight on the effects of oxygen on the BM cellular components. Here, we present simulation results that are correlated with known in vivo data of BM along with proposing a model for the two state description of allosteric hemoglobin molecule under hemolytic sickle cell anemia condition of BM.

Introduction

Hematopoiesis is the process of blood cell formation that takes place primarily in the bone marrow (BM) in adults. This produces three types of blood cells; namely, red blood cells (RBC), white blood cells (WBC) and platelets, contributing approximately one trillion cells per day to the human circulatory system.

The BM factory requires the constant availability of oxygen, the principal nutrient for the energy metabolism of active tissues. Since cessation of oxygen supply results in loss of function (BM proliferation and differentiation) within seconds, continual feed of adequate amount of oxygen to tissue is the pivotal task for nutrient delivery vehicles; the BM microcirculation. In addition, due to the intricate structure of tissue, the metabolic oxygen requirements are spatially varied and highly heterogeneous. It is for this reason that understanding the mechanism affecting the oxygen delivery to the tissue is of great importance. The experimental techniques available to-date have been inadequate for studying the oxygen concentration and its distribution within the BM due to the inaccessibility of the BM, and thus modeling provides an attractive alternative to have a better understanding of the BM function under normal and pathophysiological conditions.

In the present work, we develop models to study the oxygen transport between the extravascular space (tissue) and the delivery system of the BM. The model is essentially based on symmetry description of oxygen loading and unloading between the two conformational states of hemoglobin; deoxyhemoglobin and

oxyhemoglobin. The model is extended to study the bone marrow under pathological condition, which is sickle cell anemia in this case. The transport model under normal conditions combines oxygen transport in the sinusoidal region with the extravascular space surrounding these vessels. In addition, as the famous Hill equation has been utilized for the representation of the oxygen saturation curve, to account explicitly for the effect of pH and carbon dioxide on the oxygen transport, the variable Hill coefficient model has been implemented.

The development of such physiologically relevant models for oxygen tension distribution in the human BM could offer numerous clinical/medical applications including understanding of the effects of oxygen tension on drug efficacy (chemotherapy) to the hematopoietic compartment, and assisting in the reconstitution of *ex vivo* bone marrow engineering constructs.

Sickle Cell Anemia

Sickle cell anemia is a disorder/disease of the blood which has been subjected to intense scrutiny at the vascular, clinical, cellular, biochemical and molecular levels over the last few decades in order to have a better understanding of the pathophysiology of the disease which portends the development of effective therapy. It is an inherited disorder that is uniquely accompanied by a severe clinical phenotype of vascular occlusion. The disease, caused by inherited abnormal hemoglobin (an oxygen-carrying protein within the red blood cells), results in a sudden increase

* Corresponding author's e-mail: ahsan.islam@utoronto.ca

in the destruction of red blood cells called hemolysis (Figure 1).

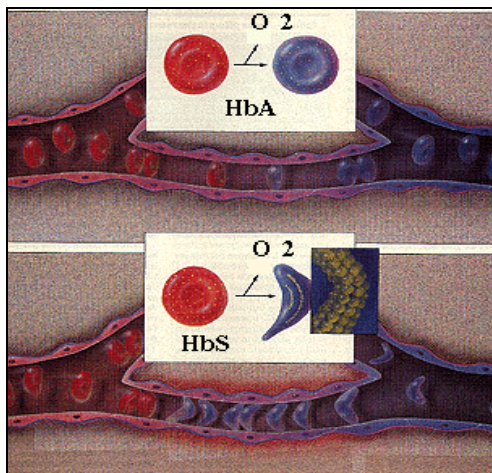


Fig 1. Normal hemoglobin (HbA) and sickle hemoglobin (HbS)³

The varied clinical manifestations of sickle cell anemia are generally attributable to either microvascular occlusion or accelerated red blood cell destruction. While possible determinants of vasocclusion have received much investigative attention, fewer studies have addressed the hemolytic component of this disease². The sickle RBCs (Fig 1) appear to be more susceptible to fragmentation and disintegration than normal RBCs. Hence, the aim of this research project is to develop a model to analyze the effect of the hemolytic rate on the oxygen distribution in the bone marrow.

Models for Allosteric Proteins

Monod and Jacob⁵ introduced the term ‘allosteric’ in a discussion on end-product inhibition. Presently, allosteric term refers to any mechanism in which protein can exist in two (or more) distinct conformations, which differ in their affinity for a ligand. More specifically, hemoglobin is an allosteric protein as the binding of oxygen at one hemoglobin site is coupled with the binding of other substances at other sites, due to the conformational change of the molecule⁹. From a mechanistic perspective, there are two hypotheses that describe the conformational changes in the allosteric molecules: the symmetry or two-state model of Monod *et al*, known as MWC model⁶ and the sequential or induced-fit model model of Koshland *et al*, known as KNF model⁷.

The MWC or two-state model of co-operativity has at its core the axiom that only a single R (Relaxed)-state

and T (Tension)-state exist, and co-operative functioning and allosteric modulation occur simply by a switching between different population distributions of the R- and T-states.

The sequential or induced-fit model involves four subunits, one binding site per subunit, and one type of ligand. The assumptions in the induced-fit model are that each subunit can exist in either of two conformational states, the A and B states, with the equilibrium constant $K_T = (B)/(A)$ characterizing the relative stability of the conformations.

Oxygen Transport in Blood

Hemoglobin is basically an iron containing pigment of vertebrate red blood cells that functions primarily in the transport of oxygen from the lungs to the tissues of the body. This molecule in almost all vertebrate is tetramer consisting of four peptide chains, each with an incorporated heme group. During the oxygenation of hemoglobin molecule, the Fe of each heme group binds O₂ molecule to cause conformational change of hemoglobin which in turn affects its ability to further bind oxygen or other molecules. The binding affinity of hemoglobin for oxygen molecule is influenced by hemoglobin-oxygen saturation (SO₂) which is defined as the fraction of available oxygen-binding sites occupied by oxygen and is expressed as either a fraction or a percent⁹.

The ability of a medium to dissolve free oxygen is characterized by a parameter called the Bunsen solubility coefficient and is denoted by α . According to Henry’s law: $[O_2] = \alpha P$ (1)

where $[O_2]$ is the concentration of dissolved oxygen and P is the partial pressure of oxygen (oxygen tension), pO_2 ⁹.

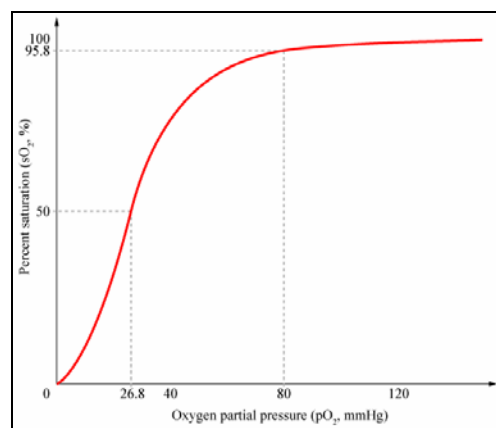
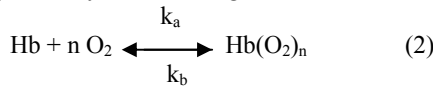


Fig 2. Oxyhemoglobin Dissociation Curve¹⁰.

The plot of oxygen-hemoglobin (Hb-O₂) saturation vs. oxygen tension (pO₂) is a sigmoid curve called Oxyhemoglobin Dissociation Curve (ODC) or Oxygen-Hemoglobin Equilibrium Curve (OHEC) (Fig 2). In order to do the mathematical modeling of oxygen transport to various tissues, accurate expressions for SO₂ as a function of pO₂ and other parameters are very important. The available expressions for describing the ODC curve fall into two categories. Those that are derived from the kinetic models of hemoglobin-oxygen reaction, and those that are constructed empirically without the aid of kinetics. In 1910, Hill proposed the first kinetic model, which expressed the sigmoidal shape of the ODC curve, can be explained by the following reaction:



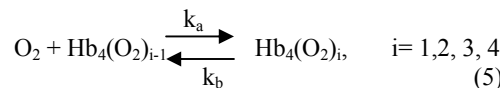
where n represents the number of molecules of oxygen that bind with hemoglobin (Hb) to form oxyhemoglobin [Hb(O₂)_n] and k_a and k_b are the association and dissociation rate coefficients, respectively. In equilibrium, the Hb saturation can be described using:

$$S = \frac{K[\text{O}_2]^n}{1 + K[\text{O}_2]^n} \quad (3)$$

where K= k_a/k_b is the equilibrium constant and [O₂] is the concentration of free oxygen in hemoglobin solution. Using Henry's law (Equation 1), we can rewrite equation 3 in the following form:

$$S = \frac{(P/P_{50})^n}{1 + (P/P_{50})^n} \quad (4)$$

where P₅₀ = 1/(Kα) is the value of pO₂ at which the hemoglobin is 50% saturated. Equation 4 is reasonably accurate within the saturation range 20 – 80% with n ≈ 2.7 for human blood. This equation is called the Hill equation⁸, its simplicity has resulted in being used within numerous mathematical simulations. However, for a more realistic presentation some authors have also applied a more complicated expression for the dissociation curve; namely the Adair's four step mechanism^{1, 11}.



In equilibrium, the above equation yields the Adair equation:

$$S = \frac{a_1 P + 2a_2 P^2 + 3a_3 P^3 + 4a_4 P^4}{4(1 + a_1 P + a_2 P^2 + a_3 P^3 + a_4 P^4)} \quad (6)$$

where S is expressed as the ratio of the number of oxygen molecules to the total number of hem groups:

$$S = \frac{\sum_{i=1}^4 i[\text{Hb}_4(\text{O}_2)_i]}{\sum_{i=1}^4 [\text{Hb}_4(\text{O}_2)_i]} \quad (7)$$

Constants a_i's are called Adair constants⁹. The mathematical complexity of the Adair's model has retarded its use in mathematical simulation of oxygen transport.

Mathematical Model

Oxygen Transport Simulation

Majority of the oxygen transport models developed to-date are usually based on the Adair type reaction scheme or its modifications, the basic equations of which are presented as^{9, 12}

$$\alpha_b \left[\frac{\partial p_b}{\partial t} + \vec{v} \cdot \nabla p_b \right] = \nabla \cdot [K_b \nabla p_b] - R \quad (8)$$

$$H_T \left[\frac{\partial \gamma}{\partial t} + \vec{v} \cdot \nabla \gamma \right] = \nabla \cdot [H_T D_H \nabla \gamma] + R \quad (9)$$

The 'R' term is the reaction term corresponding to the addition or subtraction of oxygen from the surrounding plasma. The cases analyzed in this section include: 1) the oxygen transport model with constant Hill's coefficient (Equation 10), 2) explicit expression for the carbon dioxide in the Hill's equation (Equation 11), and 3) variable Hill's coefficient (Equations 12-14). The following equations summarize these cases:

$$R = N_i k_d \left[\frac{f(p) - \gamma}{1 - f(p)} \right] \quad (10)$$

$$f(p) = \left[\frac{Kp(\text{O}_2)^n}{1 + Kp(\text{O}_2)^n} \right] \quad (11)$$

$$f(p) = \left[\frac{Kp(\text{O}_2)^n}{1 + Kp(\text{O}_2)^n + mp(\text{CO}_2)} \right] \quad (12)$$

$$f(p) = \left[\frac{K_0 p(\text{O}_2)^n}{1 + K_0 p(\text{O}_2)^n} \right] \quad (13)$$

$$K_0 = K' \left[\frac{[H^+]_{pl}}{r} \right]^L \frac{\left(1 + K_2 \left(\frac{[H^+]_{pl}}{r} \right) + (\alpha_{\text{CO}_2})_{rbc} K_6 r' \left(\frac{p\text{CO}_2}{[H^+]_{pl}} \right) \right)}{\left(1 + K_1 \left(\frac{[H^+]_{pl}}{r} \right) + (\alpha_{\text{CO}_2})_{rbc} K_3 r' \left(\frac{p\text{CO}_2}{[H^+]_{pl}} \right) \right)} \quad (14)$$

where, $K' = K_3 r^L (\alpha_{\text{O}_2})_{rbc}^n$

The variable Hill constant model and the modified Hill equation were presented by Sharan *et al.*¹⁴ and Sharan & Singh¹³, respectively. All the variables in these equations have also been defined in the nomenclature

section of this paper, and can also be found in the appropriate papers.

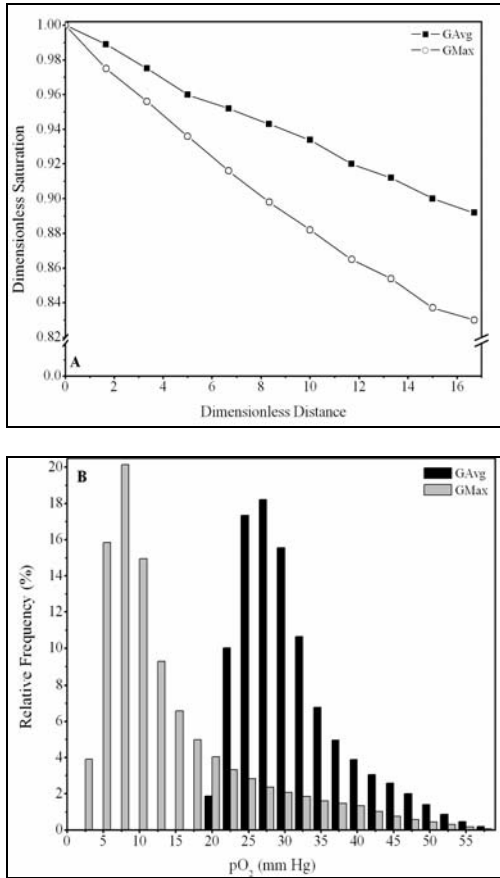


Fig 3. A. Oxygen saturation against dimensionless axial distance within the sinus. The simulation results are presented under steady state condition for maximum (GMax) and average (GAvg) granulocyte consumption rates in the homogeneous tissue environment. B. The oxygen tension distribution within the BM microenvironment for the conditions in A.

Although no quantitative verification can be offered that validates the simulation results, we can, however, present qualitative description of the oxygen transport process that does offer a partial authentication of the results. It is known that the saturation level decreases by approximately 15% during the transport process under normal conditions¹², and as can be seen in Fig 3, the saturation for the hemoglobin does decrease by 15% under maximum granulocyte consumption. The BM is a highly heterogeneous tissue with a multimodal distribution of cellular components, and in turn implying a wide variation in the consumption rate

values. The literature data is based on the consumption rates of cells in brain tissue, which has a closer oxygen uptake rate to the progenitor granulocytes than other cell types.

One of the main limitations of the Hill equation, despite its simplicity offering a tremendous advantage, is its inability to capture the ODC throughout its entire plasma oxygen partial pressure range. The above representations of the Hill equation attempts to overcome this deficiency. Figure 4 manifests a comparison between the saturation levels and the oxygen tension distribution for the different representations of the Hill equation (Equations 10-14).

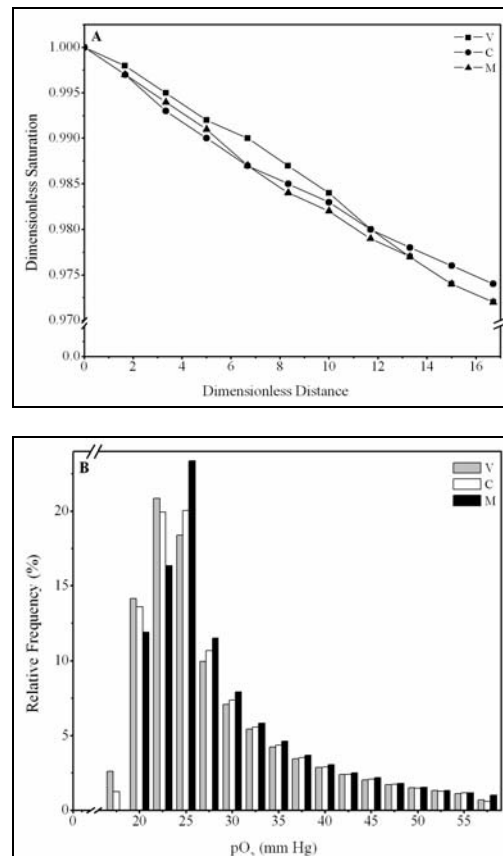


Fig 4. A. Oxygen saturation against dimensionless axial distance within the sinus. The simulation results are presented for a one residence time of blood flow and average granulocyte consumption rate. Variable Hill Coefficient (V), Constant Hill coefficient (C), and Modified Hill Equation (M). B. The oxygen tension distribution within the BM microenvironment for the conditions in A.

The results in Figure 4 shows that the variable Hill constant model predicts a lower average tissue partial

pressure and a lower oxygen distribution within the tissue environment (B), while the saturation decrease is at a slower rate than predicted by other models. Although such results can be considered to be negligible under the present circumstances, it is, however, more likely to be important under pathological conditions where any sensitivity in the model simulation can impart significant effects on the oxygen distribution in the tissue region.

In Figure 5, the transient development of the oxygen tension in the tissue is presented for four time points. As expected, during the early part of the simulation, majority of the tissue remains in hypoxic state, while some regions of the tissue can be anoxic. With increasing time, the tissue emerges from the hypoxic state and approaching the steady state oxygen tension values (indicated by rightward shift in the tissue profiles).

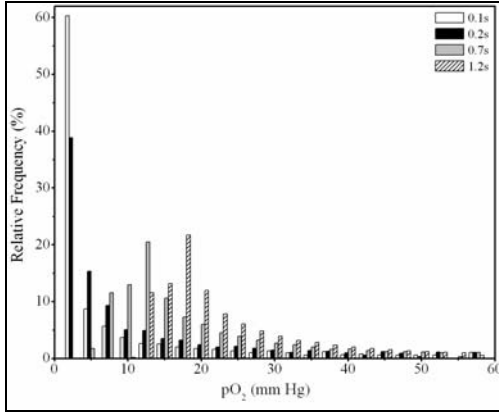


Fig 5. The transient development of oxygen tension distribution within the BM microenvironment for the conditions in Fig 4. The simulation results are presented for average granulocyte consumption rate.

Two State Model Development: Hemolysis

Alternative description to the Adair's stepwise mechanism is the two state schemes; which has been described earlier. The model presented in this section is based on the existence of the two conformational states of the hemoglobin, i.e. the oxy- and the deoxy-hemoglobin. The transport model for normal condition (Equations 15-26) is extended to hemolytic sickle cell anemia.

Sinus Region

$$\alpha_b \left[\frac{\partial p_b}{\partial t} + \vec{v} \cdot \nabla p_b \right] = \nabla \cdot [K_b \nabla p_b] - R \quad (15)$$

$$\left[\frac{\partial N_{HO}}{\partial t} + \vec{v} \cdot \nabla N_{HO} \right] = \nabla \cdot [D_H \nabla N_{HO}] + R \quad (16)$$

$$\left[\frac{\partial N_H}{\partial t} + \vec{v} \cdot \nabla N_H \right] = \nabla \cdot [D_H \nabla N_H] - R \quad (17)$$

Tissue Region

$$\alpha_t \left[\frac{\partial p_t}{\partial t} \right] = \nabla \cdot [K_t \nabla p_t] - m_0 \quad (18)$$

where

$$R = k_d \left[N_H \left(\frac{f(p)}{1-f(p)} \right) - N_{HO} \right] \quad (19)$$

$$f(p) = \left[\frac{K_0 p^n}{1 + K_0 p^n} \right] \quad (20)$$

where, k_0 = variable Hill constant¹³

$$K_b = \alpha_b D_o \quad (21)$$

$$\alpha_b = \alpha_0 \left(1 + 1.997 \times 10^{-2} [Hb] \right) \quad (22)$$

where [Hb] is in millimolars.

$$\alpha_0|_{35^\circ C} = 1.459 \times 10^{-3} \text{ mM/Torr} \quad (23)$$

$$D_H = (14032 - 95.14[Hb] + 2627[Hb]^2 - 2800[Hb]^3) \times 10^{-7} \text{ cm}^2/\text{s} \quad (24)$$

$$D_o = (2.0719 - 4.505[Hb] - 0.310[Hb]^2 + 5.1794[Hb]^3) \times 10^{-5} \text{ cm}^2/\text{s} \quad (25)$$

where [Hb] is in g/cc solution and valid at 25°C.

Boundary Conditions

$$\text{BC 1: } K_b \left. \frac{\partial p_b}{\partial r} \right|_w = K_t \left. \frac{\partial p_t}{\partial r} \right|_w \quad (26)$$

$$\text{BC 2: } p_b|_w = p_t|_w$$

$$\text{BC 3: } D_H \left. \frac{\partial N_{HO}}{\partial r} \right|_w = D_H \left. \frac{\partial N_H}{\partial r} \right|_w = 0$$

In Figure 6, the results are presented for the two state model under normal conditions. The boundary conditions for the oxy- and deoxy-hemoglobin at the sinusoidal/tissue interface maintain the total concentration of hemoglobin to be constant. During the oxygen transport process, the release of oxygen from the oxy-hemoglobin is transferred to the deoxy-hemoglobin, and to the plasma region; and the concentration gradient between the tissue and the blood drives the plasma pO_2 into the tissue region. This process is clearly demonstrated in Figure 6(A). The hemolytic model assumed random destruction of the erythrocytes and the 'death' term is present only in the equations for the oxy- and deoxy-hemoglobin.

Future Works

The hemolytic model presented in this paper is still in the early stages of development and significant amount of work is yet to be carried out to actually reach a point where a working model is attained; but mathematical modeling represents an excellent alternative to examining the pathological implications of sickle hemoglobin and the related changes in the bone marrow oxygen transport.

Given that, at present, only a simplified model for the RBC destruction has been considered, it is fitting that we advance the model so that more realistic features of the *in vivo* sickle cell disease are captured involving both the intravascular and extravascular destruction of erythrocytes.

The model advancements can proceed on three major fronts: microcirculation structure, extravascular arrangement of cellular components, fluid dynamics of the blood flow and its components and RBC destruction mechanism. Accounting for all these factors would indeed formulate a more complete model that can lead to true predictions of the disease.

However, such a model would be appropriate for a long-term research goal, but for the immediate case, we propose features that can be incorporated into the present hemolytic model from the aspects of using CFD software CFX. To account for the propensity for RBC interaction with macrophages, we propose a multiphase model that includes both RBCs and macrophages and under certain conditions, this can lead to RBC hemolysis. To account for the extravascular destruction of the RBC, the heterogeneous geometrical presentation can be extended to include random destruction of cellular components through the use of source terms.

As a final point, although the strategy is yet undetermined, the hemolysis model can be combined with Sickle Cell polymerization aspects; such a model is a step towards the real *in vivo* situation.

Acknowledgement

The author would like to thank Commonwealth Scholarship Commission for funding the project.

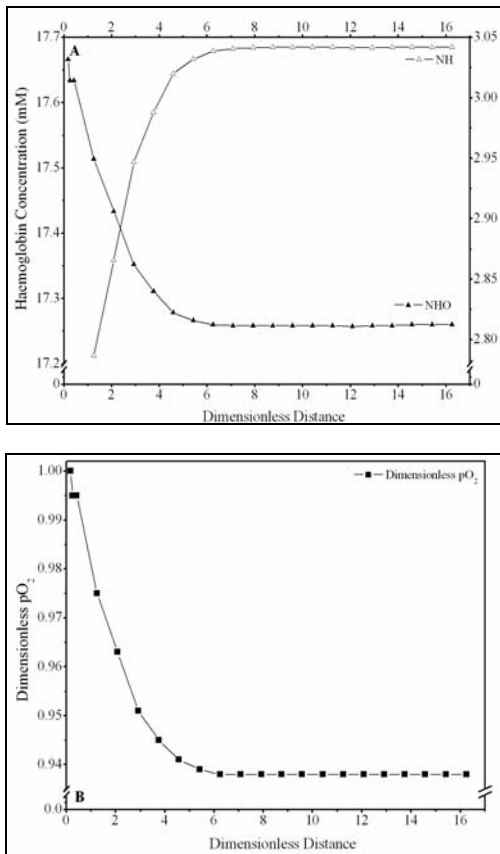


Fig 6. A. The variation in concentration of oxy- and deoxy-hemoglobin for normal oxygen transport, against dimensionless axial distance within the sinus. The simulation results are presented at 0.75s and average granulocyte consumption rate. The Hill constant with Variable Hill Coefficient (V), is utilized in the model above. B. The axial variation in oxygen tension conditions within the vessel. Further model parameters are presented in Appendix.

Nomenclature

D_b	Diffusion coefficient of blood in tissue	cm^2s^{-1}
D_t	Diffusion coefficient of oxygen in tissue	cm^2s^{-1}
D_H	Diffusion coefficient of hemoglobin in blood	cm^2s^{-1}
M	Modified Hill Constant for CO_2	1/mmHg
m_0	Volumetric oxygen consumption rate	$\text{mol O}_2 \text{cm}^{-3}\text{s}^{-1}$
K	Equilibrium Constant	cm^3g^{-1}
K_{eff}	Effective Krogh coefficient	$\text{mol O}_2 \text{cm}^{-3}\text{s}^{-1} \text{mmHg}^{-1}$
k_d	Dissociation rate coefficient	-
k_a	Association rate coefficient	-
K_b	Oxygen permeability-blood	$\text{mol O}_2 \text{cm}^{-3}\text{s}^{-1} \text{mmHg}^{-1}$
K_t	Oxygen permeability-tissue	$\text{mol O}_2 \text{cm}^{-3}\text{s}^{-1} \text{mmHg}^{-1}$
K_m	Michaelis-Menten Constant	mmHg
n	Hill's Coefficient	-
N_H	Molar concentration of oxyhemoglobin	$\text{mol Hb cm}^{-3} \text{blood}$
N_H	Molar concentration of deoxyhemoglobin	$\text{mol Hb cm}^{-3} \text{blood}$
N_T	Molar concentration of total hemoglobin	$\text{mol Hb cm}^{-3} \text{blood}$
S	Sink or source term	$\text{mol O}_2 \text{cm}^{-3}\text{s}^{-1} \text{mmHg}^{-1}$
R	Consumption rate	$\text{mol O}_2 \text{cm}^{-3}\text{s}^{-1} \text{mmHg}^{-1}$
$[\text{H}^+]$	Hydrogen ion concentration	nmol/cm^3
pl	Plasma	-
p_t	Oxygen Tension in tissue	mm Hg
p_b	Oxygen Tension in blood	mm Hg

Greek Symbols

α_b	Oxygen solubility-blood	$\text{mol O}_2 \text{cm}^{-3} \text{mm Hg}^{-1}$
α_t	Oxygen solubility-tissue	$\text{mol O}_2 \text{cm}^{-3} \text{mm Hg}^{-1}$
μ	Viscosity	p
ρ	Density	gcm^{-3}
Γ	Diffusion coefficient	-
γ	Oxygen saturation function	-
λ	Thermal conductivity	-
ϕ	General variable	-

References

1. Adair, G.S., The Hemoglobin System. VI. The oxygen dissociation curve of hemoglobin. *J Biol. Chem*, 63: 529-545, 1925.
2. Bensinger, T.A. and Gillette, P.N., Hemolysis in sickle cell disease. *Arch Intern Med* 133:624-631, 1974.
3. Bwh. Harvard, : *What is sickle cell disease?* http://sickle.bwh.harvard.edu/scd_background.html, 2002
4. Changeux, J-P and Edelstein, SJ, Allosteric receptors after 30 years. *Neuron*, 21: 959-980, 1998.
5. Monod, J. and Jacob, F., General conclusions: telenomic mechanisms in cellular metabolism, growth and differentiation. *Cold Spring Harbor Symp Quant Biol* 26:389-401, 1961.
6. Monod, J., Wyman, J., and Changeux, J-P, On the nature of allosteric transitions: a plausible model. *J Mol Biol* 12:88-118, 1965.
7. Koshland, D. E., Nemethy, G., and Filmer, D., Comparison of experimental binding data and theoretical models in proteins containing subunits. *Biochemistry* 5:365-385, 1966.
8. Hill, A.V., The possible effects of the aggregation of the molecules of hemoglobin on its dissociation curve. *J. Physiol* (London), (iv): 41, 1910.
9. Popel, A.S., Theory of Oxygen Transport to Tissue, *Critical Reviews in Biomedical Engineering*, 17(3): 257-321, 1989.
10. Wikipedia, Hemoglobin <http://en.wikipedia.org/wiki/Hemoglobin>, 2004
11. Yap, EW, Hellums, J.D., Use of Adair four-step kinetics in mathematical simulation of oxygen transport in the microcirculation. *Adv Exp Med Biol.*, 215: 193-207, 1987.
12. Groebe, K. and Thews, G., Basic mechanisms of diffusive and diffusion-related oxygen transport in biological systems: a review. *Advances in Experimental Medicine and Biology*. 317(Oxygen Transport to Tissue XIV): 21-33, 1992.
13. Sharan, M., and Singh, M.P., Equivalence between one step kinetics and Hill's Equation. *J Biomed Eng* 6: 297-302, 1984.
14. Singh, M.P., Sharan, M. and Aminataei, A., Development of mathematical formulae for O_2 and CO_2 dissociation curves in the blood. *IMA J Math Appl Med Biol* 6:25-46, 1989.